

Interfacial Polycondensation Encapsulation in Miniemulsion

L. Torini,[†] J. F. Argillier,[‡] and N. Zydowicz^{*,†}

Laboratoire des Matériaux Polymères et Biomatériaux, UMR CNRS 5627,
Université Claude Bernard Lyon 1, 69622 Villeurbanne Cedex, France, and
Institut Français du Pétrole, 92852 Rueil Malmaison Cedex, France

Received October 22, 2004; Revised Manuscript Received January 28, 2005

ABSTRACT: Oily core polyurethane nanocapsules with a mean diameter of 200 nm were formulated in miniemulsion by interfacial polycondensation. The encapsulation process in miniemulsion was optimized by the choice of the surfactant type (anionic, cationic, or nonionic) and concentration; hexadecane was the costabilizer. Size distribution was studied by dynamic laser light scattering, and ζ potential was also determined. The size distribution appeared relatively narrow. Scanning and transmission electron microscopy experiments attested for the submicrometer size, the spherical shape of the capsules, and a smooth external wall. The thermal properties of the polyurethane wall were determined by DSC and TGA, with a fusion temperature around 40 °C, suggesting the presence of defects in the macromolecular backbone such as irregular bounds of urethane and urea functions. The chemical structure of the polymer wall was studied by ^{13}C NMR and MALDI–TOF mass spectrometry. Both methods attested for the presence of urethane and urea units in the macromolecular chain. MALDI–TOF experiments allowed the investigation of the microstructure of the polymer wall and proved the presence of urethane and urea homopolymer and urethane–urea copolymer. Although the determination of the molecular weight was not possible because of the high polydispersity of the sample, the mass range was comprised between 500 and 3000 Da, in accordance with the number-average molecular weight determined by size exclusion chromatography (PS standards).

Introduction

Miniemulsions are dispersions of relatively stable oil droplets with a size range 50–500 nm in water, prepared by shearing a system containing oil, water, surfactant and costabilizer (or hydrophobe).¹ When carefully prepared, polymerizations in such miniemulsions result in latex particles which have about the same size as the initial droplets.² This means that the appropriate formulation of a miniemulsion suppresses the coalescence of droplets and Ostwald ripening and a virtually one to one copying process of the droplets to the particles concerning their size can be obtained.

Polymerization of the oil droplets of such miniemulsions turned out to be very promising,² compared to the emulsion polymerization heavily restricted in radical copolymerization or other polymer reaction, leading to the formation of polymer latexes. In miniemulsion polymerization, the concept of “nanoreactors” allowing the formation of polymer latex particles ideally in a 1:1 copying process, is realized. Furthermore, it was recently shown that the process of miniemulsion is excellently suited to perform a variety of reactions in dispersed media and to prepare stable latexes and the principle of miniemulsion polymerization can be transferred to polyadditions.^{3–5}

The control of the morphology of latex particles has been an important area in polymer science. Technology has advanced such that a variety of structured particles are nowadays accessible. Synthetic methods leading to polymer particles having cavities and voids have also been extensively investigated. Such particles are currently named nanocapsules. The potential value of nanocapsules has been discussed for a variety of phar-

maceutical and cosmetic applications, such as medium for controlled release.^{6,7}

Nanocapsule size is usually lower than 1 μm . However, for more and more applications, especially in medicine, smaller capsules between 50 and 300 nm are of high interest. The approach for synthesis of nanocapsules described below is based on the principle of miniemulsion by interfacial polycondensation. Up to now, this kind of process has never been used for the synthesis of nanocapsules, even if polyester and polyurethane or epoxy nanoparticles have been already prepared by miniemulsion polyaddition.^{3,5,6} We describe in this paper the formation of polyurethane nanocapsules, composed of an organic liquid core and a polymer shell with mean diameter of 200 nm. The influence of various parameters such as the choice of the surfactant type (anionic, cationic or nonionic) and its concentration, the ratio surfactant to costabilizer were examined. The thermal properties of the polyurethane wall were determined by DSC and TGA and the chemical structure of the polymer wall was studied by ^{13}C NMR and MALDI–TOF mass spectrometry. MALDI–TOF experiments allowed us to study the microstructure of the polymeric membrane, and showed a mass range in accordance with the average molecular weight determined by size exclusion chromatography (PS standards).

Experimental Section

Chemicals. Cyclohexane, hexadecane (HD), 1,6-hexanediol (HDOH), isophorone diisocyanate (IPDI), sodium dodecyl sulfate (SDS), cetyltrimethylammonium chloride (CTACl, 25% in water) and cetyltrimethylammonium bromide (CTABr), poly(vinyl alcohol), 88% hydrolyzed (PVA, $M_n = 22\,000$ g/mol), and sodium bis(2-ethylhexyl) sulfosuccinate (Na(AOT)) were purchased from Aldrich and used as received.

SE 1010 copolymer (styrene–ethylene oxide) was kindly supplied by Goldschmidt AG.

* To whom correspondence should be addressed.

[†] Université Claude Bernard Lyon 1.

[‡] Institut Français du Pétrole.

Nanocapsule Preparation. For preparing the miniemulsion, 0.66 g of SDS (3 wt % relative to the organic dispersed phase) were added to 70 g of deionized water. After the surfactant dissolution, 0.66 g of hexadecane were added, and the mixture was stirred for 1 h at 50 °C. Then 10 g cyclohexane containing 2.22 g of IPDI (0.01 mol), a slowly reacting cyclic isocyanate, were added under magnetic stirring to the aqueous phase, and the magnetic stirring was kept for 5 min. The pH of the aqueous phase was measured in order to verify the isocyanate function hydrolysis. The miniemulsion is then prepared by ultrasonifying the emulsion for 180 s at 60% amplitude (Branson sonifier W750 digital). Then 10 g of water containing 5.9 g of HDOH (0.05 mol) were added drop to drop for 1 min under ultrasonifying at 20% amplitude. The temperature was then increased to 40 °C under magnetic stirring (1000 rpm) for 4 h.

The slowly reacting behavior of the IPDI is interesting in this application, as it should not react significantly with water which composed the continuous phase of the miniemulsion.

Cyclohexane is used in our experiments as the oil for the oil-filled nanocapsules, and does not play any role in the reaction except solubilizing the IPDI.

The nanocapsules were separated by centrifugation at 9000 rpm, redispersed in a small volume of distilled water, and after lyophilisation they were obtained as powder. The powder was dissolved in the accurate solvent for the MALDI-TOF, ¹³C NMR, and SEC experiments.

Analysis. Scanning electron microscopy (SEM) experiments were performed on a Hitachi S800 at 10 kV after coating with gold-palladium (Hummer II Coater). Transmission electron microscopy (TEM) experiments were performed on a Philips CM 120 at 80 kV. A droplet of the aqueous nanocapsule solution was deposited on copper grids with Formvar film. The excess solution was removed.

Thermal Gravimetric Analysis. Samples weighing 2–10 mg were heated at 10 °C/min from 25 °C to 250 °C in a stream of helium in the microbalance of a TGA 2950 Du Pont Instruments thermal gravimetric analyzer.

Differential Scanning Calorimetry. Samples weighing 5–10 mg were heated from –80 to +250 °C in sealed capsules in a stream of helium in the oven of a DSC 2920 Modulated DSC TA Instruments. First run: 25–250 °C. Cooling 10 °C/min. Second run: –80 °C to +150 °C.

Size Exclusion Chromatography. Polymeric membrane was analyzed on Styragel columns (10³ and 10⁵ Å) connected to a Waters 410 (Waters-Millipore) differential refractometer, using DMF as solvent.

The size distribution of the nanocapsules was determined by dynamic laser light scattering on a Zetasizer NanoZS 90 that was kindly supplied by Malvern Instruments.

¹³C NMR Spectroscopy. ¹³C NMR spectra of nanocapsules were recorded on a Bruker DRX 400 spectrometer (100.25 MHz for ¹³C) in DMSO-*d*₆ at 298 K. The pulse angle was 70°, and the delay time was 10 s for the spectra recorded in quantitative conditions.

MALDI-TOF Mass Spectrometry. MALDI-TOF (matrix-assisted laser desorption ionization-time-of-flight) MS experiments were conducted using a VOYAGER DE-STR from Perkin-Elmer equipped with a N₂ laser (λ = 337 nm), with dithranol as matrix. The spectra were recorded in reflectron mode over the range 500–3 000 with salt addition (NaI). The solvent was DMSO. External calibration was performed with PEG, giving a precision of 0.05%.

FTIR Spectroscopy. The reagents and the nanocapsules were analyzed on a Perkin-Elmer 1760-X spectrometer by combining them in KBr pellets.

Results and Discussion

Stability of the Miniemulsions. In previous experiments,⁵ the application of the miniemulsion process was described to synthesize polyurethane dispersions with diameters of about 200 nm in a one-step procedure. PU particles were formed by the miniemulsification of a

monomer mixture of IPDI and 1,6-hexanediol in an aqueous surfactant solution followed by heating. We propose an original method for nanocapsule formation based on the interfacial polycondensation of these both monomers. The original procedure starts with the preparation of a stable miniemulsion with the internal phase containing one of the monomers, as it is commonly used for the preparation of microcapsules by interfacial polycondensation.^{8–10} The single difference lies in the use of a costabilizer, or cosurfactant, added to the surfactant. The term of cosurfactant is rather misleading, because in most cases, the agent is not a cosurfactant in the traditional sense, as it is not an amphiphile at all.¹¹ The use of a small percentage of costabilizer allows to build up an osmotic pressure in the droplets which provides stability against Ostwald ripening. Once the stable miniemulsion obtained, the second monomer dissolved in the external phase is added to the miniemulsion, and the reaction between the both monomers occurs at the interface of the two nonmiscible phases.

The costabilizers described in the literature are such as cetyl alcohol, hexadecane,^{12,13} or dodecyl mercaptan.¹⁴ The efficiency of the costabilizer is reported to be dependent on its chemical nature.^{15,16} It was noted that hexadecane produced a much finer droplet size than cetyl alcohol and that the average drop size does not change as a function time when it was used as the costabilizer. In our case, the use of cetyl alcohol was not considered because of the side reaction between its hydroxyl group and the isocyanate groups. Thus, the chemical nature and character of the hydrophobic additive was not examined here, and hexadecane was used as costabilizer.

Even the influence of cationic and nonionic surfactants was recently examined,¹¹ miniemulsion recipes are mostly based upon the anionic sodium dodecyl sulfate (SDS) as surfactant.^{17,18} Thus, our experiments started with SDS as surfactant. First of all, we were interested in the formation and characterization of miniemulsion, without the polycondensation reaction subsides at the interface of the droplets.

Influence of the Miniemulsion Preparation Mode.

In the first set of experiments, SDS was used at a concentration equal to 3 wt % of the organic phase with a surfactant-to-costabilizer ratio of 1:1, and we investigated the effect of the preparation mode on the miniemulsion characteristics.

There are several methods to prepare miniemulsions depending on the type of surfactant and costabilizer used, and the volume of the miniemulsion desired.^{15,19,20} Delgado²¹ explains that the choice of optimum emulsification method is dependent on the total volume of the miniemulsion to be prepared. Small volume requires the dissolution of the costabilizer in the oil phase and the dissolution of the surfactant in the aqueous phase. As regards hexadecane as costabilizer, some authors recommend its dissolution in the oil phase,¹⁵ whereas others recommend its dispersion in the aqueous phase containing the surfactant.²⁰ Anyway, the chemical structure of hexadecane cannot lead to the formation of an interfacial stabilizing complex with SDS, as it is reported for cetyl alcohol.²²

Our basic recipe for the preparation of miniemulsion is based on the dispersion of hexadecane in the aqueous phase with the surfactant. Experiments were also performed with hexadecane dissolved in the oil phase

Table 1. Z-average Diameter, Polydispersity Index (PDI), and Electrokinetic Potential (ζ) of the Miniemulsions According to the Preparation Mode

sample preparation	surfactant type	[surfactant] (wt %)	surfactant-to-cosurfactant ratio	Z-average diameter (nm)	PDI	ζ (mV)
dissolution of the costabilizer in the organic phase	SDS	3	1:1	153	0.12	-87
dispersion of the costabilizer in the aqueous phase	SDS	3	1:1	196	0.08	-68

Table 2. Z-Average Diameter, Polydispersity Index (PDI) and Electrokinetic Potential (ζ) of the Miniemulsions and the Polyurethane Nanocapsules According to the Surfactant Concentration^a

surfactant type	[surfactant] (wt %)	surfactant-to-costabilizer ratio	sample	Z-average diameter (nm)	PDI	ζ (mV)
SDS	3	1:1	mini-emulsion	196	0.08	-68
			nanocapsules	186	0.11	-96
SDS	2	1:1	mini-emulsion	208	0.21	-94
			nanocapsules	191	0.07	-95
SDS	1	1:1	mini-emulsion	183	0.34	-74 ^b
			nanocapsules	201	0.19	-86 ^c

^a Nanocapsules were synthesized at 40 °C during 4 h. ^b Phase separation after 1 week. ^c Flocculation after 1 week.

Table 3. Z-Average Diameter, Polydispersity Index (PDI), and Electrokinetic Potential (ζ) of the Miniemulsions and the Polyurethane Nanocapsules According to the Surfactant Type^a

surfactant type	[surfactant] (wt %)	surfactant-to-costabilizer ratio	sample characteristics	Z-average diameter (nm)	PDI	ζ (mV)
SDS	3	1:1	nanocapsules	196	0.08	-68
AOT	3	1:1	nanocapsules	337	0.06	-40
CTACl	3	1:1	nanocapsules	<i>b</i>	<i>b</i>	<i>b</i>
CTABr	3	1:1	mini-emulsion	<i>b</i>	<i>b</i>	<i>b</i>
SE1010	1.6	1:1	nanocapsules	<i>c</i>	<i>c</i>	<i>c</i>

^a Nanocapsules were synthesized at 40 °C during 4 h. ^b Phase separation or Flocculation after 12 h. ^c Flocculation after a few days.

in order to investigate the influence of the costabilizer locus on the stability and the size of the miniemulsion droplets.

The features of the miniemulsions obtained in each case, are quite similar (Table 1). The miniemulsion prepared with hexadecane dissolved in the oil phase, presents a z-average diameter equal to 153 nm and a broader size distribution compared to the results obtained for miniemulsions prepared with HD dispersed in the aqueous phase. The ζ potentials of the miniemulsions are quite close, suggesting the same electrostatic repulsions between the droplets.

Influence of the Surfactant Concentration. Colloidal stability is usually controlled by the type and amount of the employed surfactant. In miniemulsion, the fusion–fission rate equilibrium during sonification and therefore the size of the droplets directly after primary equilibration depend on the amount of surfactant. The surfactant concentration commonly ranges between 1 and 5 wt % relative to the monomer. In our experimental conditions, the surfactant concentration is relative to the dispersed organic phase (cyclohexane).

The miniemulsions were prepared with HD dispersed in the aqueous phase. Decreasing SDS concentration from 3 to 1 wt % does not effectively change the droplet size (Table 2), that remains around 200 nm, but the size distribution becomes broader, especially with SDS concentration of 1 wt %. Furthermore, a phase separation appeared after 1 week for this miniemulsion, whereas the miniemulsions prepared with SDS concentrations of 2 and 3 wt % remain stable over than several months. Furthermore, diameter and ζ -potential measurements were steadily performed and attested to the colloidal stability.

The ζ potential of the miniemulsions measured immediately after their preparation cannot explain the particular instability of the miniemulsion prepared with 1 wt % SDS.

The influence of the surfactant concentration was also verified on the stability of the polyurethane nanocapsules (Table 2). The observations were the same as with the miniemulsions. Whereas the nanocapsules prepared with 2 and 3 wt % SDS concentrations remain stable over 18 months, flocculation rapidly occurs in the sample prepared with 1 wt %. These results show the importance of the miniemulsion stability on the performance of the nanocapsule formation process.

Influence of the Surfactant Type. Practically all miniemulsion recipes are based upon the anionic surfactant SDS that seems to provide the most stable miniemulsions. However, for a number of applications, cationic and nonionic surfactants are required. Anionic and cationic surfactants have been reported for the formation of monodispersed droplets between 30 and 200 nm; nonionic oligomeric or polymeric surfactants are suitable for the formation of droplets between about 100 and 800 nm.²³

After the first step experiments based on the use of SDS as surfactant, we wanted to check the efficiency of another widely used and efficient anionic surfactant, i.e. AOT, at an amount of 0.66 g (3 wt % relative to the dispersed phase) and a weighted surfactant-to-costabilizer ratio equal to 1:1.

The influence of the surfactant nature was studied on nanocapsules obtained by interfacial polycondensation. Stable nanocapsules were prepared with a mean diameter around 340 nm (Table 3), slightly higher than for the previously synthesized nanocapsules with SDS (196 nm). The ζ potential of the nanocapsules was found equal to -40 mV, close to the value obtained with SDS, attesting to the same particle surface coverage.

Contrarily to Landfester's results with styrene as monomer,¹¹ cationic surfactants such CTABr and CTACl did not allow one to stabilize the polyurethane nanocapsules that flocculated 12 h later. Intended for determining the origin of the instability of these nano-

Table 4. Z-Average Diameter, Polydispersity Index (PDI), and Electrokinetic Potential (ζ) of the Miniemulsions and the Polyurethane Nanocapsules According to the Surfactant to Costabilizer Ratio

sample characteristics	surfactant type	reaction temp (°C)	reaction duration (h)	[surfactant] (wt %)	surfactant-to-costabilizer ratio	Z-average diameter (nm)	PDI	ζ (mV)
miniemulsion	SDS			3	1:1	196	0.08	-68
miniemulsion	SDS			3	1:3	160	0.15	-99
nanocapsules	SDS	40	4	3	1:1	186	0.11	-96
nanocapsules	SDS	25	1.5	3	1:3	154	0.21	-103

capsules, a miniemulsion was prepared with 3 wt % CTABr. This miniemulsion presented a phase separation 12 h after its preparation, suggesting that CTABr is not efficient in our experimental conditions.

The nonionic surfactant SE1010 presents two kinds of difference compared to the previous ones. It is a nonionic surfactant, and it is a copolymer of ethylene oxide and styrene. Its HLB value was estimated equal to 10, which is relatively low to ensure an efficient stabilization of the direct miniemulsion. It was used at a lower concentration equal to 1.6 wt %, because its lower solubility in water. It provided the formation of larger size capsules with a broad size distribution that flocculated a few days later.

As a conclusion on the influence of the surfactant type on the colloidal stability, anionic surfactants such as SDS and AOT, allowing high electrostatic repulsion between the particles, appear the most efficient, compared to the cationic and nonionic surfactants. Nevertheless, the lowest size of the miniemulsion is provided by SDS.

Influence of the Costabilizer Concentration. Hexadecane belongs to the insoluble additive family which permits stability against Ostwald ripening.^{24–26} Such molecules are effectively trapped within the droplets, and small admixtures of hexadecane or dodecane increased substantially the stability of hexane emulsions. This has the immediate consequence that no droplet of the disperse phase can ever entirely evaporate, providing that the total number of droplets remains constant in time, with a value determined by the initial conditions. Generally, for simplicity, the trapped species are treated as dilute within each droplet²⁵ and will contribute to the droplet's chemical potential. This additional term corresponds physically to the osmotic pressure of the trapped phase.

$$\Delta\mu = \left[\frac{2\sigma}{R} - \frac{\eta k_B T}{(4\pi/3)R^3} \right] \quad (1)$$

where $\Delta\mu = \mu_d - \mu_b$, μ_d is the chemical potential of the dispersed phase, μ_b is the chemical potential in a bulk liquid of the dispersed phase, η is the number of trapped particles in the droplet, R is the droplet radius, and σ is the surface tension.

Thus, the osmotic pressure of the trapped species (second term) competes directly with the Laplace pressure (first term). The latter favors fewer larger droplets whereas the osmotic pressure favors an uniform droplet size (at least if all droplets have the same η). Kabalnov et al.^{26,27} paid much attention to Ostwald ripening and discussed its quantitative regularities in a two-component disperse phase. A sufficiently high content of the costabilizer leads to the retardation of Ostwald ripening in the system. The rate of particle growth is expressed as $\omega = d\bar{a}^3/dt$, being in the case related to the respective rates for pure components ω_1 and ω_2 , and to the volume fractions of the two components in the dispersed phase, φ_1 and φ_2 by $\omega = (\varphi_1/\omega_1 + \varphi_2/\omega_2)^{-1}$.

Some emulsification studies using hexadecane as costabilizer^{13,21} demonstrated that the higher the hexadecane amount up to a certain value, the smaller the droplet size of the miniemulsion. However, the broad particle size distribution of latexes prepared by the miniemulsion process is essentially unchanged regardless of the costabilizer concentration and emulsification time. Concurrently, some other studies^{20,25,28} reported for miniemulsion polymerization no significant dependence upon the concentration of additive. Different explanations are proposed. Landfester²⁰ suggests that directly after the miniemulsification, the pressure balance is not obtained. Fontenot and Shork²⁹ observed no optimum ratio of costabilizer to surfactant when HD is used, unlike miniemulsions prepared with fatty alcohol costabilizers. They relied this fact to the absence of any interaction between the surfactant and costabilizer. Welin and Berger²⁸ showed that the needed costabilizer amount depends on the droplet size distribution of the emulsion and the disperse phase volume. The efficiency of the ripening inhibitor was directly correlated to its solubility in the dispersed phase and the experimentally observed rates of increase in droplet size were closely correlated with those predicted according to the Lifshitz–Slezov–Wagner theory.

The influence of the surfactant-to-costabilizer ratio with a SDS concentration of 3 wt % was investigated. We observed that a ratio equal to 1:1 provided the formation of droplets with a z-average diameter of 196 nm, instead of 160 nm for miniemulsion obtained with a 1:3 ratio (Table 4). This diameter difference is not significant. Nevertheless, the size distribution of the latter miniemulsion was slightly higher with a polydispersity index of 0.15 instead of 0.08 for the 1:1 miniemulsion.

The influence of the costabilizer amount was also examined on nanocapsules obtained after interfacial polycondensation (Table 4). Similar results were obtained with no significant diameter differences.

Comparison between Miniemulsion Droplet and Nanocapsule Size. The main interest of miniemulsion process consists of the fact that the miniemulsion droplets are polymerized without changing their identity.¹ Nevertheless, the formation of nanocapsules by interfacial polycondensation in miniemulsion relies on a different reaction mechanism than the radical polymerization. As regards this difference, we wanted to determine the evolution of the mean diameter during the interfacial polycondensation process. The encapsulation process begins with the formation of a primary membrane induced by the interfacial reaction of IPDI and 1,6-hexanediol. The growth of this membrane will then depend on the diffusion of the hydrophilic monomer (diol) through the swelled membrane toward the organic phase. The kinetics of the polymeric membrane formation is then diffusion-controlled. The requirement of a perfectly stable state of the interface is definitely necessary, at least during the formation of the primary membrane.

Table 5. Z-Average Diameter and Polydispersity Index (PDI) of the Polyurethane Nanocapsules According to the Surfactant to Reaction Temperature and Reaction Time

surfactant type	reaction temp (°C)	reaction duration (h)	[surfactant] (wt %)	surfactant-to-costabilizer ratio	Z-average diameter (nm)	PDI
SDS	25	4	3	1:1	154	0.21
SDS	40	4	3	1:1	186	0.11
SDS	40	4	3	1:1	177	0.11
SDS	50	4	3	1:1	196	0.12
SDS	60	4	3	1:1	185	0.13
SDS	40	24	3	1:1	227	0.15

The evolution of the mean diameter during the polycondensation process was followed under various experimental conditions.

Laser light scattering measurements of miniemulsions obtained with different SDS concentrations ranging between 1 and 3 wt %, with a surfactant-to-costabilizer ratio of 1:1, present the same size distribution profiles and the same z-average diameters as the corresponding nanocapsules (Table 2). The same observations were made with the experiments performed with a SDS concentration equal to 3 wt % and surfactant-to-costabilizer ratio of 1:1 and 1:3 (Table 4).

We can conclude that the identity of the miniemulsion droplets is preserved during the interfacial polycondensation process at the interface. This important fact attests for the reliable use of the miniemulsion process in the formation of polycondensate nanocapsules.

Synthesis of the Nanocapsules. IPDI was dissolved in cyclohexane as dispersed organic phase. The organic phase is added to the aqueous phase of SDS containing dispersed hexadecane, under magnetic stirring during 5 min and pH was systematically monitored in order to estimate the hydrolysis of the NCO groups during the emulsification process. pH systematically ranges between 6.80 and 7.20, suggesting the absence of NCO hydrolysis during this first step, in accordance with the slowly reacting behavior of the IPDI, compared to more reactive isocyanates such as 1,6-diisocyanatohexane or 4,4'-methylenabis(phenylisocyanate). The ultrasonification time was chosen equal to 3 min which induces a reduced temperature increase ($T_{\max} = 42\text{ }^{\circ}\text{C}$). The turbidity of the preparation increases very rapidly in the first seconds of ultrasonification, becomes milky and then remains constant. The sonification amplitude is then decreased to 20% during the drop to drop addition of the 1,6-hexanediol aqueous solution to the miniemulsion. The reaction then subsides under magnetic stirring during 4 h at 40 °C. The functional groups (isocyanate to hydroxy groups) were employed in a 1:5 molar ratio, corresponding to an excess of alcohol functions which is often required by the interfacial polycondensation process^{8,9,33} due to the required diffusion of the hydrophilic monomer into the organic phase.

First of all, the reproducibility of the encapsulation reaction was verified in terms of size and size distribution with a SDS concentration equal to 3 wt % and a surfactant-to-costabilizer ratio of 1:1 (Table 5) at 40 °C during 4 h. In these conditions, nanocapsules with a z-diameter around 186 nm and a polydispersity index equal to 0.11 were obtained. They were observed by SEM and TEM (Figure 1, parts a and b). Both techniques attested to the presence of submicrometer capsules.

The external wall of the nanocapsules appeared smooth (Figure 1a), in accordance with the typically observed morphology of the external wall of microcapsules obtained by an interfacial polycondensation

process from normal emulsion (H/E).^{33,34} The morphology of the external wall is explained by the formation mechanism and kinetics of the primary membrane. Many parameters can influence the interfacial polycondensation kinetics. The reactivity of the both monomers,³⁵ the viscosity of the external phase depending on the molecular weight and the chemical structure of the diol^{30,31} and the nature of the dispersed phase. The latter must concurrently induce the precipitation and the swelling of the growing membrane. The low reactivity of the aliphatic diisocyanate IPDI, compared to the aromatic TDI, will induce the formation of completely spherical capsules with clear and smooth surfaces.³⁵ The

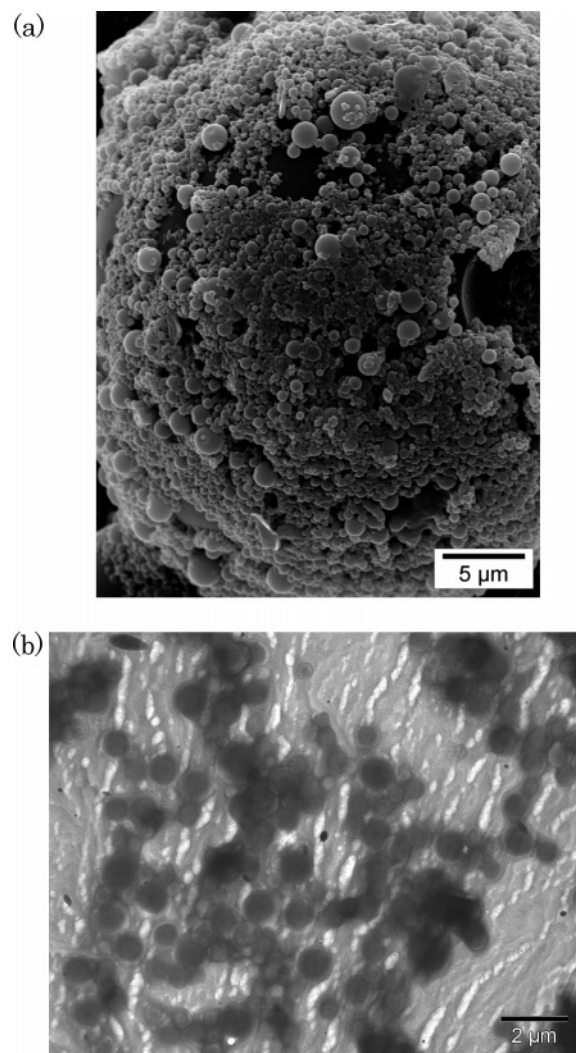


Figure 1. (a) Scanning electron micrograph of polyurethane nanocapsules prepared at 40 °C during 4 h with 3 wt % SDS and surfactant-to-costabilizer ratio of 1:1. (b) Transmission electron micrograph of polyurethane nanocapsules prepared at 40 °C during 4 h with 3 wt % SDS and surfactant-to-costabilizer ratio of 1:1.

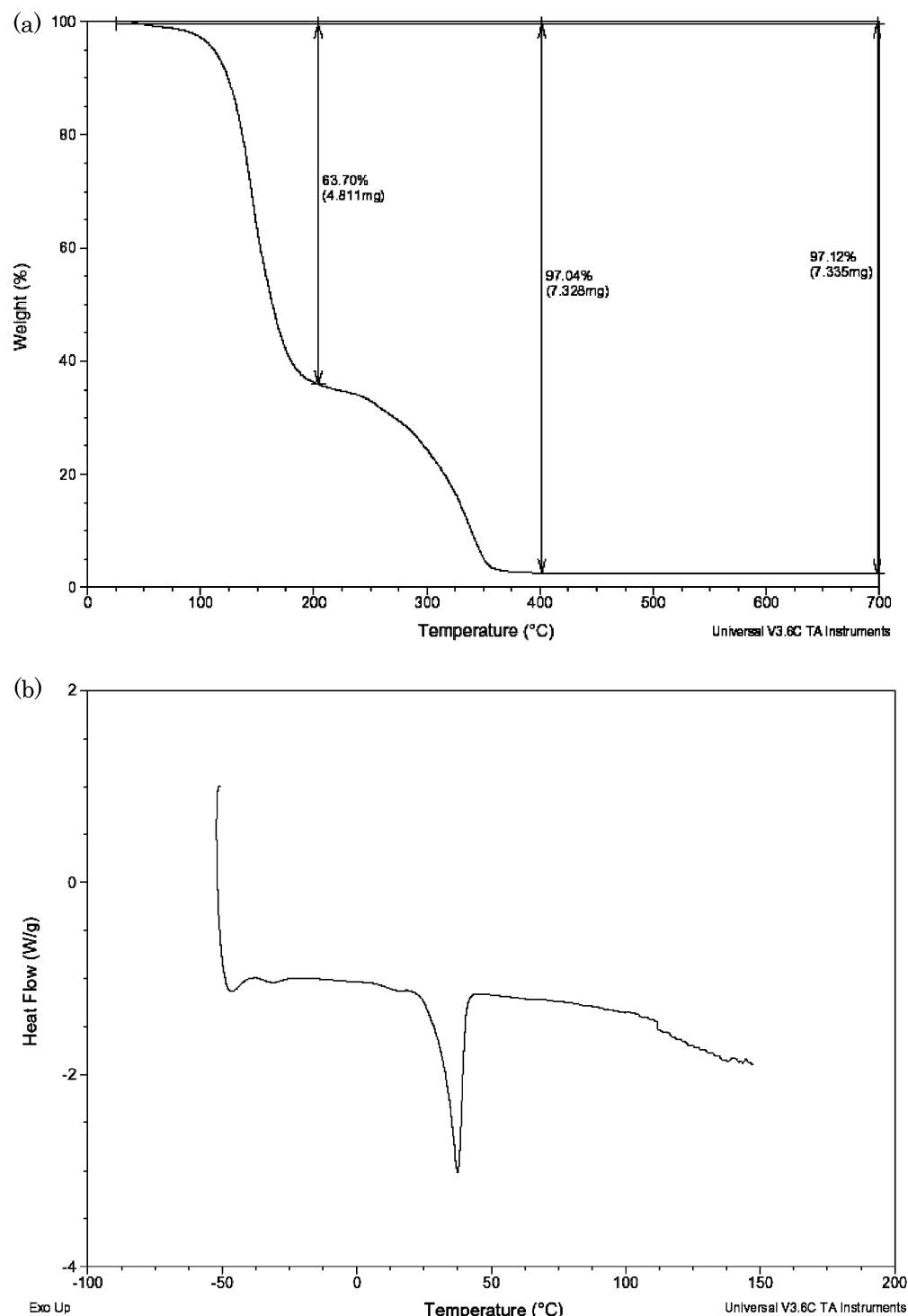


Figure 2. (a) Thermal behavior of polyurethane nanocapsule wall prepared at 40 °C during 4 h with 3 wt % SDS and surfactant-to-costabilizer ratio of 1:1. Ramp temperature: 10 °C/min. (b) Dynamic scanning calorimetry of polyurethane nanocapsule wall prepared at 40 °C during 4 h with 3 wt % SDS and surfactant-to-costabilizer ratio of 1:1. Ramp temperature: 10 °C/min. First run: from 30 to 200 °C. Second run: from -80 to +150 °C.

length of the diol will also influence the morphology of the capsules. For example, 1,6-hexanediol will induce smoother surface than ethylene glycol. Microcapsules prepared with ethylene glycol present more permeable holes in the wall because of its shorter chain.³⁵ Thus, the spherical shape and the smooth surface of the nanocapsules observed by scanning electron microscopy are in accordance with the literature and our experimental conditions.

Influence of the Temperature. Besides the molecular diffusion of the dispersed phase, the destabilization

of an emulsion can also occur by a collision and coalescence process.

Temperature is an important parameter in the emulsion process. A change in temperature causes many changes in the physicochemical properties of the emulsified system such as the interfacial tension between the two phases, the nature and viscosity of the interfacial film, the relative solubility of the emulsifying agent in the two phases, the vapor pressure and viscosity of the liquid phase, and finally the thermal agitation of the dispersed particles. Changes can be such

that emulsion inversion or break can occur. Anyway, this problem is rarely mentioned in the papers concerning radical polymerization in miniemulsion. Styrene polymerization classically subsides at 70 °C,²⁰ acrylic acid, acrylamide, and hydroxyethyl methacrylate are polymerized in inverse miniemulsions with cyclohexane at 65 °C with span 80 as surfactant.³²

In interfacial polycondensation process, the interfacial stability is very important^{8,33} because the polymeric membrane formation must begin from the liquid–liquid interface between the internal and external phase. If the droplet surface is not well stabilized, the formation of the polymeric membrane will not occur at the interface, capsules will not be obtained, and a phase separation will occur as soon as the stirring is stopped.

The influence of the temperature and reaction time on the size and size distribution of the polyurethane nanocapsules was then investigated.

Nanocapsules were synthesized at 40, 50, and 60 °C during 4 h with a SDS concentration of 3 wt % and a surfactant-to-costabilizer ratio of 1:1. Higher reaction temperature was not allowed because of the boiling point of cyclohexane equal to 80.7 °C. No significant difference on the size and size distribution was underscored between the various reaction times (Table 5), once more suggesting the efficiency of SDS for this application.

An experiment was performed at 40 °C during 24 h. It seems that a long reaction time induces the broadening of the size distribution and the increase of the size of the nanocapsules (Table 5).

Thermal Properties of Nanocapsules. Thermal properties of nanocapsules were investigated using TGA and DSC. Figure 2a presents the TG diagram of the nanocapsules. The sample shows the first weight loss of about 65% at 200 °C, the second one reaches 32.5% between 200 and 400 °C. The polymer is completely degraded at 400 °C. The first weight loss was deemed to be due to the bounded water departure, the second one to the decomposition of the polyol segments. A third weak inflection point at 250 °C could correspond to the breakup of some urea–urethane segments. These characteristics are in accordance with microcapsule polyurethane thermal properties.^{34,35}

The typical second run of the DSC experiments of the PU nanocapsules is shown in Figure 2b.

This essentially shows a main feature: a strong endotherm at 38.5 °C due to melting of soft segments. This value of melting temperature is in accordance with some reported results.^{34–37} Nevertheless, a strict comparison cannot be established, because the papers deal with segmented polyurethane obtained mostly from macrodiols and chain extender. The thermal properties of these polyurethanes rely especially on the ratio of hard to soft segments and phase separation phenomena. The relatively low value of melting temperature of our polyurethane nanocapsule wall could be explained by the presence of defaults in the macromolecular backbone such as irregular bounds of urethane and urea units.

No glass temperature is observed in the experimental conditions of DSC experiments. A low molecular weight of the polyurethane and/or the absence of segmented chains could provide a T_g that is too low to be observed in our thermal conditions.

Kinetics of the Polycondensation Reaction. Influence of the Duration and the Temperature. Interfacial polycondensation encapsulation processes

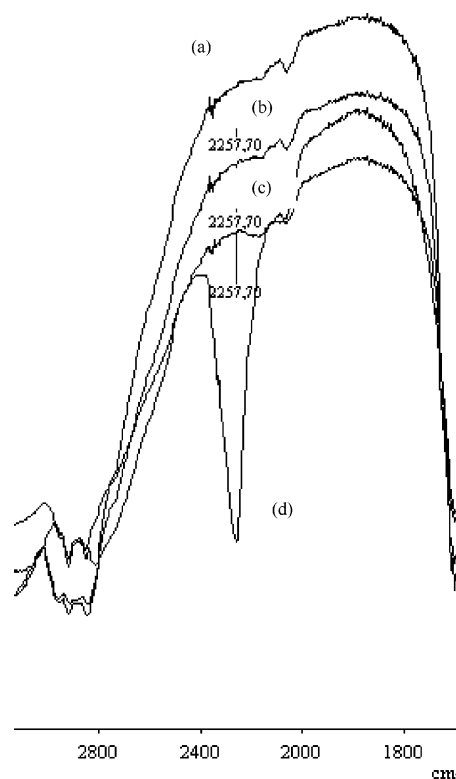


Figure 3. FTIR spectra of polyurethane nanocapsule wall: (a) $T = 40$ °C; (b) $T = 50$ °C; (c) $T = 60$ °C; (d) $T = 25$ °C.

commonly do not require high reaction temperatures. Low temperatures such room temperature are interesting from the process easiness point of view. Nevertheless, the reaction must be completed at the end of the process.

The reaction completion is followed by FTIR by the evolution of the vibration band at 2250 cm^{-1} , corresponding to the NCO functions. Some residual isocyanate functions are observed when the reaction subsides at 25 °C during 4 h. The intensity decrease of the NCO vibration band at 2250 cm^{-1} is only observed at temperature higher than 40 °C during 4 h (Figure 3).

MALDI–TOF Mass Spectrometry. MALDI–TOF is a relatively new mass spectrometry technique and the most promising method for the ionization of large molecules and the analysis according to their molar mass and functionality.^{38,39} Compared to other mass spectrometric techniques, the accessible mass range has been extended considerably. The instrumental resolution is sufficient to separate oligomer peaks of low molecular weight polymers ($<10\,000\text{ Da}$). Thus, an accurate mass analysis to the individual oligomers can bring some information on repeat unit, end group and polymer modifications.³⁸ Thus, MALDI–TOF MS is a complementary spectral method of NMR spectroscopy. This method is rarely reported for the study of polymers obtained by interfacial polycondensation.⁸

Figure 4a shows the MALDI–TOF mass spectrum of the nanocapsule wall prepared at 40 °C during 4 h with a SDS concentration of 3 wt % and a surfactant-to-costabilizer ratio of 1:1.

Many peaks are apparent between m/z 500 and 3000. Because of the non Gaussian profile of the mass distribution, the average molecular mass cannot be estimated, but the observed mass range is in accordance with the SEC-calculated M_n equal to $4370\text{ g}\cdot\text{mol}^{-1}$ ($M_w/M_n = 1.98$; PS standards).

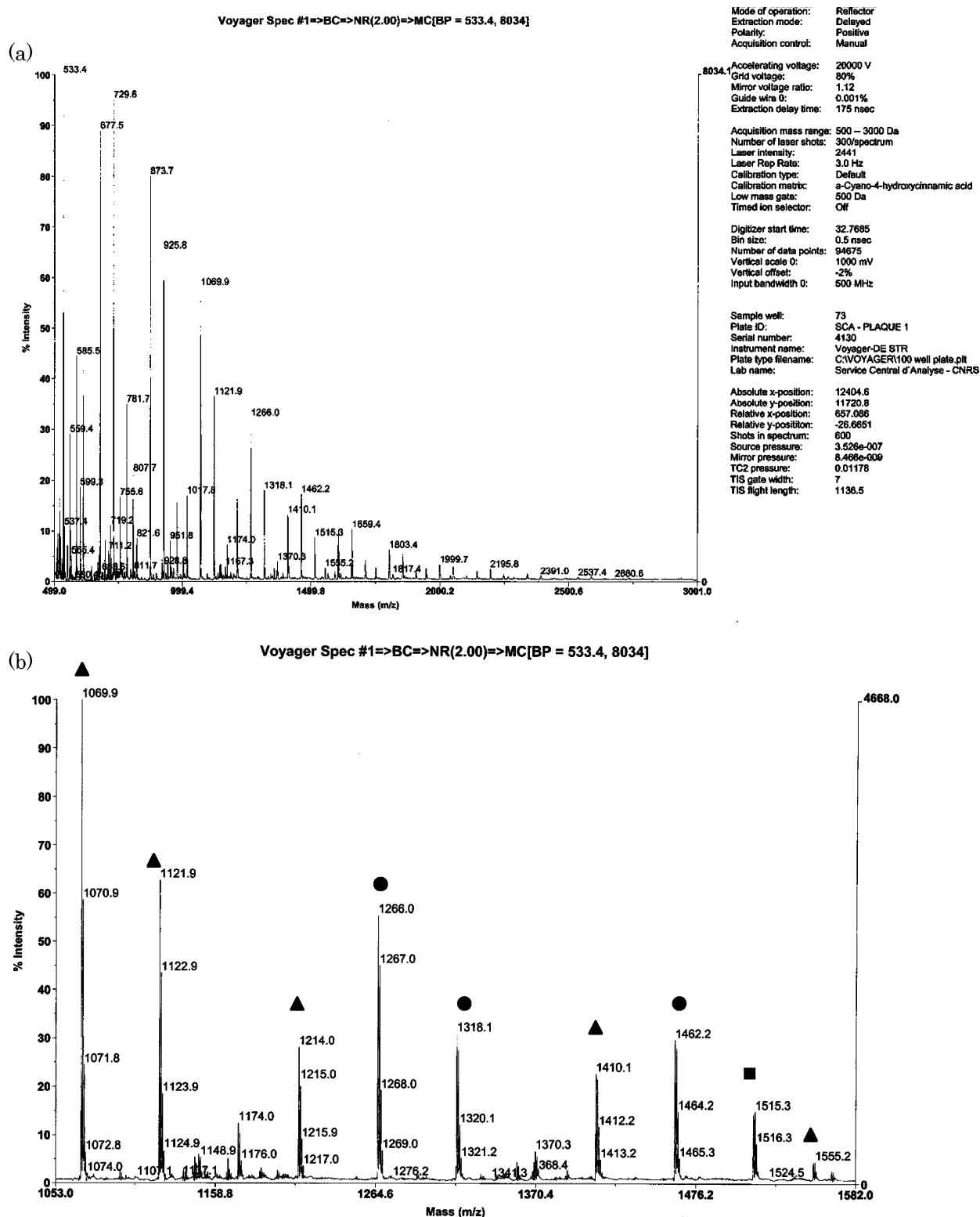


Figure 4. (a) MALDI-TOF mass spectrometry spectrum of polyurethane nanocapsule wall prepared at 40 °C during 4 h with 3 wt % SDS and surfactant-to-costabilizer ratio of 1:1. (b) MALDI-TOF mass spectrometry expanded spectrum of polyurethane nanocapsule wall prepared at 40 °C during 4 h with 3 wt % SDS and surfactant-to-costabilizer ratio of 1:1. Enlargement of the (1050–1580 Da) spectral region. Key: (■) urethane homopolymer; (▲) urea homopolymer; (●) urea-urethane copolymer.

Figure 4b shows the enlarged spectrum from m/z 1050 to 1580. The m/z values of the most intense peaks do not show regular differences, attesting to a complex chemical microstructure of the polymer. The main reaction between IPDI and 1,6-hexanediol induces the formation of a polyurethane backbone. But even if the

side reaction kinetics of IPDI with water is slower than with 1,6-hexanediol, the hydrolysis of the NCO functions of IPDI during the polycondensation process providing the formation of urea functions, is unavoidable in our experimental conditions. Thus, the characterization of the spectrum was based on the assumption that the

Table 6. Experimental and Calculated m/z Values of Cationized (MNa^+) Species According to the Repeat Unit^a

Species	n	MNa^+ calculated average mass (Da)	MNa^+ experimental average mass (Da)
$R = \left[\begin{array}{c} -\text{C}-\text{NH}-\text{C}_9\text{H}_{16}-\text{CH}_2-\text{NH}-\text{C}-\text{O}-(\text{CH}_2)_6-\text{O}- \\ \parallel \quad \parallel \\ \text{O} \quad \text{O} \end{array} \right]_n$			
$\text{HO}-(\text{CH}_2)_6-\text{O}-\text{R}-\text{H}$	2	821.5616	821.6
$\text{H}_2\text{N}-\text{CH}_2-\text{C}_9\text{H}_{16}-\text{NH}-\text{R}-\text{H}$	1	533.4043	533.4
	2	873.6405	873.7
	3	1213.8767	1214.0
	4	1554.1129	1554.2
$\text{H}_2\text{N}-\text{CH}_2-\text{C}_9\text{H}_{16}-\text{NH}-\text{R}-\text{CO}-\text{NH}-\text{C}_9\text{H}_{16}-\text{CH}_2-\text{NH}_2$	1	729.5618	729.6
	2	1069.7980	1069.9
	3	1410.0342	1410.1
	4	1750.2704	1750.4
$\text{OCN}-\text{CH}_2-\text{C}_9\text{H}_{16}-\text{NH}-\text{R}-\text{CO}-\text{NH}-\text{C}_9\text{H}_{16}-\text{CH}_2-\text{NCO}$	1	781.5204	781.7
	2	1121.7566	1121.9
	3	1461.9928	1462.2
	4	1802.2290	1802.4
	5	2142.4652	2142.7
$R' = \left[\begin{array}{c} -\text{NH}-\text{C}_9\text{H}_{16}-\text{CH}_2-\text{NH}-\text{C}- \\ \parallel \\ \text{O} \end{array} \right]_n$			
$\text{H}-\text{R}'-\text{NH}-\text{C}_9\text{H}_{16}-\text{CH}_2-\text{NH}_2$	2	585.4831	585.5
	3	781.6406	781.7
	4	977.7981	977.9
	5	1173.9556	1174.0
	6	1370.1131	1370.3
$\text{H}-\text{R}'-\text{O}-(\text{CH}_2)_6-\text{OH}$	2	533.4042	533.4
	3	729.5617	729.6
	4	925.7192	925.8
	5	1121.8767	1121.9
	6	1318.0342	1318.1
	7	1514.1917	1514.3
	8	1710.3492	1710.5
$\text{HO}-(\text{CH}_2)_6-\text{O}-\text{R}'-\text{O}-(\text{CH}_2)_6-\text{OH}$	2	677.4828	677.5
	3	873.6403	873.7
	4	1069.7978	1069.9
	5	1265.9553	1266.0
	6	1462.1128	1462.2
	7	1658.2703	1658.4
	8	1854.4278	1854.5
	9	2050.5853	2050.7
Urea-urethane unit *			
$\text{OCN}-\text{CH}_2-\text{C}_9\text{H}_{16}-\text{NH}-\text{R}_2-\text{R}'_1-\text{NH}-\text{C}_9\text{H}_{16}-\text{CH}_2-\text{NCO}$		1017.719	1017.8
$\text{OCN}-\text{CH}_2-\text{C}_9\text{H}_{16}-\text{NH}-\text{R}_4-\text{R}'_2-\text{NH}-\text{C}_9\text{H}_{16}-\text{CH}_2-\text{NCO}$		2194.544	2194.8
$\text{OCN}-\text{CH}_2-\text{C}_9\text{H}_{16}-\text{NH}-\text{R}_2-\text{R}'_2-\text{NH}-\text{C}_9\text{H}_{16}-\text{CH}_2-\text{NCO}$		1514.0715	1514.2
$\text{OCN}-\text{CH}_2-\text{C}_9\text{H}_{16}-\text{NH}-\text{R}_1-\text{R}'_2-\text{NH}-\text{C}_9\text{H}_{16}-\text{CH}_2-\text{NCO}$		1854.3077	1854.5
$\text{OCN}-\text{CH}_2-\text{C}_9\text{H}_{16}-\text{NH}-\text{R}_4-\text{R}'_2-\text{NH}-\text{C}_9\text{H}_{16}-\text{CH}_2-\text{NCO}$		2194.544	2194.8
$\text{HO}-(\text{CH}_2)_6-\text{O}-\text{CO}-\text{R}_1-\text{R}'_5-\text{O}-(\text{CH}_2)_6-\text{OH}$		1606.1915	1606.3
$\text{HO}-(\text{CH}_2)_6-\text{O}-\text{CO}-\text{R}_1-\text{R}'_7-\text{O}-(\text{CH}_2)_6-\text{OH}$		1998.5065	1998.6
$\text{HO}-(\text{CH}_2)_6-\text{O}-\text{CO}-\text{R}_2-\text{R}'_5-\text{O}-(\text{CH}_2)_6-\text{OH}$		1946.4277	1946.5

^a Key: *R₂ means that there are two R units. R'₁ means that there is one R' unit.

macromolecular chains of the polymer are composed on one hand of urethane units, and on another hand of urea units, and even of urethane-urea units, with various ending such as NH₂, OH and NCO.

All the detected peaks could be assigned by using a complete list of m/z values, a part of which is shown in Table 6.

The m/z values were calculated by using the formula shown below:

• m/z of the chains composed of urethane units (U species):

$$m/z = L + 340.2362n + R$$

where L and R correspond to the theoretical isotopic mass of the chemical structure of the chain endings (Table 6) and n corresponds to the number of urethane units in the chain.

• m/z of the chains composed of urea units (u species):

$$m/z = L + 196.1575n' + R$$

where L and R correspond to the theoretical isotopic mass of the chemical structure of the chain endings (Table 6) and n' corresponds to the number of urea units in the chain.

• m/z of the chains composed of urethane-urea units:

$$m/z = L + 340.2362n + 196.1575n' + R$$

where L and R correspond to the theoretical isotopic mass of the chemical structure of the chain endings (Table 6), and n and n' correspond to the number of urethane and urea units respectively in the chain.

We can also point out the right accordance between the experimental and theoretical isotopic mass (Table

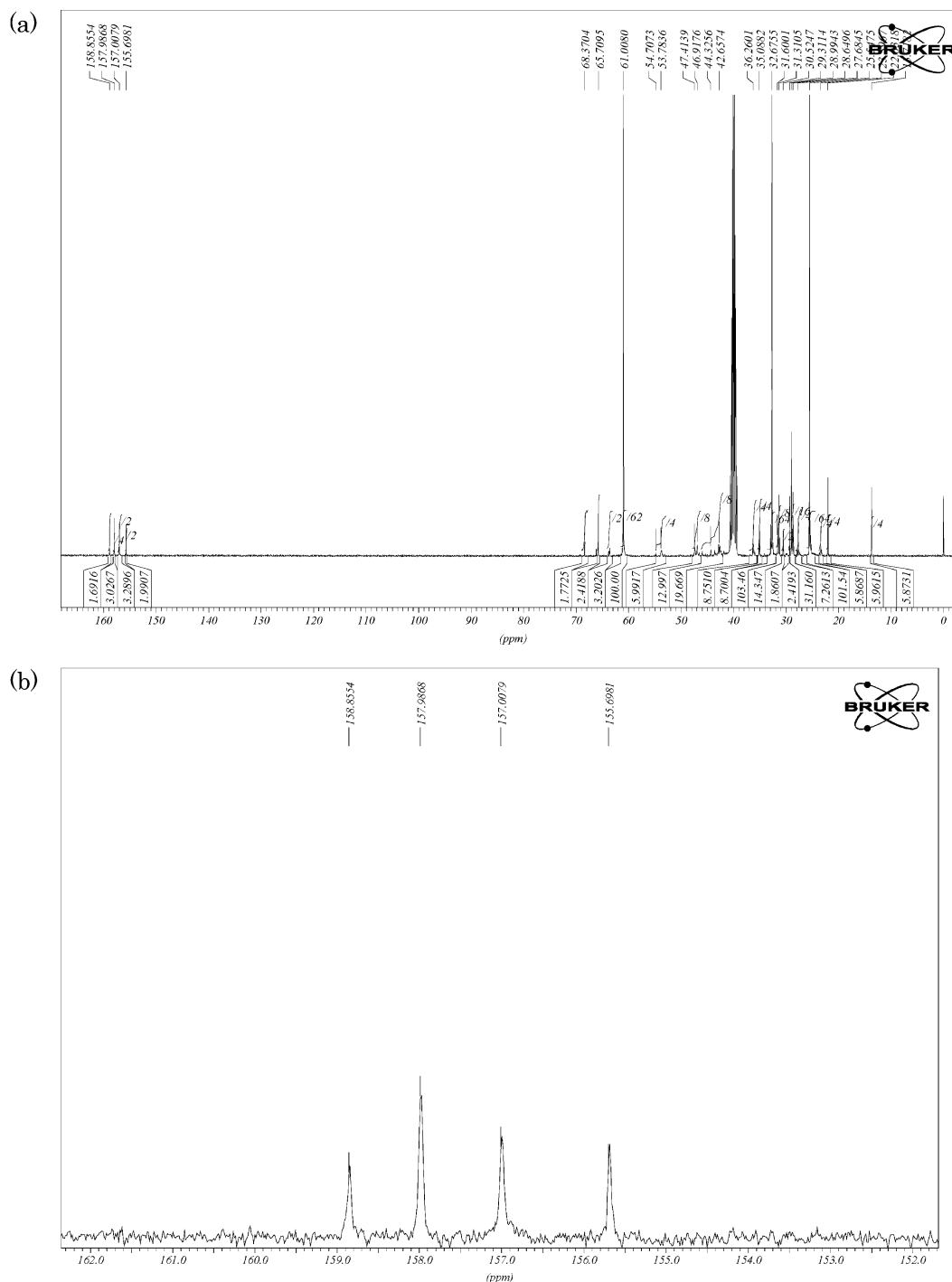


Figure 5. (a) ^{13}C (100.25 MHz) NMR spectrum of polyurethane nanocapsule wall prepared at 40 °C during 4 h with 3 wt % SDS and surfactant-to-costabilizer ratio of 1:1. (b) ^{13}C (100.25 MHz) NMR expanded spectrum of polyurethane nanocapsule wall prepared at 40 °C during 4 h with 3 wt % SDS and surfactant-to-costabilizer ratio of 1:1. (160–150 ppm) carbonyl region.

6), confirming the accuracy of the MALDI–TOF technique for the examination of the polymeric microstructure.

NMR Spectroscopy of Nanocapsules. The polymeric wall of the nanocapsules prepared at 40 °C during 4 h with a SDS concentration equal to 3 wt % and a surfactant-to-costabilizer ratio of 1:1 were analyzed by ^{13}C NMR spectroscopy under experimental quantitative conditions.

To allow the most accurate analysis of the ^{13}C NMR spectrum of the polyurethane wall, IPDI ^{13}C NMR

spectrum was also recorded. It surprisingly presents two carbonyl resonances at 122.3 and 121.4 ppm, whereas the results of the IPDI isocyanate carbonyl chemical shift modeling (Chem Draw Ultra 8.0.3) only indicate one resonance at 122.7 ppm. These two peaks correspond to the cis–trans isomer forms of the commercial IPDI sample. The isomer composition of IPDI sample involved in the formation of the polyurethane wall was then calculated and found equal to 1:1.

The ^{13}C NMR spectrum of the polyurethane wall (Figure 5a) presents two main regions corresponding to

Table 7. Chemical Structures Provided from IPDI Isocyanate Reaction and ^{13}C NMR Theoretical Chemical Shifts

Chemical structure	Theoretical chemical shift $\delta(\text{ppm})$	
	$\delta(\text{C}1) = 18.8$ $\delta(\text{C}2) = 47.8$ $\delta(\text{C}3) = 16.4$ $\delta(\text{C}4) = 46.9$ $\delta(\text{C}5) = 39.3$ $\delta(\text{C}6) = 42.0$	$\delta(\text{C}7) = 22.6$ $\delta(\text{C}8) = 27.5$ $\delta(\text{C}9) = 27.5$ $\delta(\text{C}10) = 54.5$ $\delta(\text{C}11) = 122.2$ $\delta(\text{C}12) = 122.2$
	$\delta(\text{C}1) = 18.2$ $\delta(\text{C}2) = 49.1$ $\delta(\text{C}3) = 22.4$ $\delta(\text{C}4) = 48$ $\delta(\text{C}5) = 38.9$ $\delta(\text{C}6) = 42.9$	$\delta(\text{C}7) = 22.8$ $\delta(\text{C}8) = 27.9$ $\delta(\text{C}9) = 27.9$ $\delta(\text{C}10) = 46.5$ $\delta(\text{C}11) = 156$ $\delta(\text{C}12) = 155.7$
	$\delta(\text{C}1) = 17.4$ $\delta(\text{C}2) = 48.7$ $\delta(\text{C}3) = 22.0$ $\delta(\text{C}4) = 47.6$ $\delta(\text{C}5) = 39.5$ $\delta(\text{C}6) = 42.1$	$\delta(\text{C}7) = 22.4$ $\delta(\text{C}8) = 27.9$ $\delta(\text{C}9) = 27.9$ $\delta(\text{C}10) = 47.1$ $\delta(\text{C}11) = 157.7$ $\delta(\text{C}12) = 157.7$
	$\delta(\text{C}1) = 17.8$ $\delta(\text{C}2) = 48.7$ $\delta(\text{C}3) = 22.4$ $\delta(\text{C}4) = 48$ $\delta(\text{C}5) = 38.9$ $\delta(\text{C}6) = 42.5$	$\delta(\text{C}7) = 22.4$ $\delta(\text{C}8) = 27.9$ $\delta(\text{C}9) = 27.9$ $\delta(\text{C}10) = 47.1$ $\delta(\text{C}11) = 157.7$ $\delta(\text{C}12) = 155.7$
	$\delta(\text{C}1) = 17.8$ $\delta(\text{C}2) = 49.1$ $\delta(\text{C}3) = 22.0$ $\delta(\text{C}4) = 47.6$ $\delta(\text{C}5) = 39.5$ $\delta(\text{C}6) = 42.5$	$\delta(\text{C}7) = 22.8$ $\delta(\text{C}8) = 27.9$ $\delta(\text{C}9) = 27.9$ $\delta(\text{C}10) = 46.5$ $\delta(\text{C}11) = 156.0$ $\delta(\text{C}12) = 157.7$

aliphatic carbons (70–10 ppm) and carbonyl ones (160–150 ppm). The former is composed of numerous resonances whereas the latter shows only four resonances.

The important feature of the ^{13}C NMR spectrum of the nanocapsule wall relies on the absence of the carbonyl resonances of IPDI (122.3 and 121.4 ppm), suggesting that either all isocyanate functions reacted, or the amount of residual isocyanate functions is so low that they are not detected by ^{13}C NMR spectroscopy. As mass spectrometry is well-known to be more sensitive than ^{13}C NMR spectroscopy, we can then conclude the accordance between the ^{13}C NMR and MALDI-TOF results. The latter pointed out some species with isocyanate chain ending corresponding to minor peaks (Table 6).

Excluding side reactions that occur at higher temperatures, there are various chemical functions resulting from isocyanate reactions, except the expected urethane linkages, i.e. primary amines and urea functions. The presence of such functions were underscored by mass spectrometry and can also be observed in NMR spectrum if sufficiently intense. Table 7 presents the

various possible chemical structures contained in the polymeric wall of nanocapsules from IPDI chemical structure.

The complete spectrum is relatively complex as all aliphatic resonances are comprised on a reduced spectral region between 70 and 20 ppm (Figure 5a). This complexity is increased by the presence of the cis-trans isomer structures from IPDI. Nevertheless, the enlargement of the carbonyl region shows only four distinct resonances located at 158.8, 158.0, 157.0, and 155.7 ppm (Figure 5b). The carbonyl chemical shift modeling of various structures obtained by IPDI reactions gives only three different chemical shifts at 155.7, 156.0, and 157.7 ppm corresponding respectively to urethane carbonyl (C12), urethane carbonyl (C11) and urea carbonyl (C12 and C11). Surprisingly, (C11) and (C12) carbonyls in urea units have the same chemical shift (157.7 ppm), whereas the (C11) and (C12) urethane carbonyls present a slight chemical shift difference ($\Delta\delta = 0.3$ ppm). From these values, the carbonyl resonances can be ascribed. As the cis-trans isomer structures of IPDI are in the proportion 1:1, this molar ratio should be also verified

in the structures provided from IPDI. The relative intensities of the carbonyl resonances at 158.8, 158.0, 157.0, and 155.7 ppm are respectively 100, 234, 194, and 124, suggesting that the peaks at 158.8 and 155.7 ppm correspond to the cis-trans isomer urethane (C12) and (C11) carbons. The peaks at 158.0 and 157.0 ppm should correspond to cis-trans isomer urea (C12) and (C11) carbons. As regards this hypothesis, the relative molar amount of urethane and urea groups can be assessed, and is found to be equal to 34% and 66% respectively. No more information can be obtained from the ^{13}C NMR spectrum of nanocapsule wall because of the too high complexity of the aliphatic region.

FTIR spectroscopy confirms the presence of urethane and urea groups in the nanocapsule wall with three main vibration bands at 1700, 1650, and 1550 cm^{-1} corresponding respectively to stretching of CO secondary urethane, stretching of CO urea and CHN deformation. Nevertheless, no quantitative information can be determined from FTIR experiments because of the insufficient spectral resolution.

Conclusion

We have shown that interfacial polycondensation of IPDI and 1,6-hexanediol in cyclohexane-water mini-emulsions stabilized with SDS resulted in stable polyurethane nanocapsules with a diameter around 200 nm and narrow size distributions. A critical SDS concentration higher than 1 wt %, relative to the organic dispersed phase, is required to ensure the stability of the miniemulsions and nanocapsules. Hexadecane was used as costabilizer, and the surfactant-to-costabilizer ratio, comprised between 1:1 and 1:3, has no influence on the size and size distribution of the miniemulsions and nanocapsules. The nanocapsules obtained in such conditions are stable over 18 months, without any increase of the z -average diameter and the ζ potential of the nanocapsules. The interfacial polycondensation process does not disturb the emulsion stability and does not change the droplet identity, in accordance with polymerization process in miniemulsion. The morphology of the nanocapsules was examined by SEM and TEM which confirmed the results obtained by LLS. Nanocapsules are especially spherical with smooth surface. The thermal properties of the nanocapsule wall are in accordance with polyurethane ones. Finally, ^{13}C NMR and MALDI-TOF mass spectrometry experiments confirmed the presence of urethane, urea and urea-urethane sequences in the nanocapsule polymeric wall.

References and Notes

- (1) El-Aasser, M. S.; Miller, C. M. In *Polymeric Dispersions: Principles and Applications*; Assua, J. M., Ed.; Dordrecht, The Netherlands, 1997; p 109.
- (2) Landfester, K. *Top. Curr. Chem.* **2003**, *227*, 75–123.
- (3) Barrère, M.; Landfester, K. *Polymer* **2003**, *44*, 2833–2841.
- (4) Bechthold, N.; Tiarks, F.; Willert, M.; Landfester, K.; Bechthold, M.; Antonietti, M. *Macromol. Symp.* **2000**, *151*, 549–555.
- (5) Tiarks, F.; Landfester, K.; Antonietti, M. *J. Polym. Sci.* **2001**, *39*, 2520–252.
- (6) Tasset, Ch.; Barrete, N.; Thysman, S.; Keteslegers, J. M.; Lemoine, D.; Préat, V. *J. Controlled Release* **1995**, *33*, 23.
- (7) Bouchemal, K.; Briançon, S.; Bonnet, I.; Perrier, E.; Fessi, H.; Zydowicz, N. *Int. J. Pharm.* **2004**, *269*, 89–100.
- (8) Soto-Portas, M. L.; Chaumont, P.; Zydowicz, N. *J. Membr. Sci.* **2001**, *189* (1), 41–58.
- (9) Frère, Y.; Danicher, L.; Gramain, P. *Eur. Polym. J.* **1998**, *34* (2), 193–199.
- (10) Soto-Portas, M. L.; Chaumont, P.; Zydowicz, N. *Polym. Int.* **2003**, *52* (4), 522–527.
- (11) Landfester, K.; Bechthold, N.; Tiarks, F.; Antonietti, M. *Macromolecules* **1999**, *32*, 2679–2683.
- (12) Ugelstad, J.; El-Aasser, M. S.; Vanderhoff, J. W. *J. Polym. Sci., Polym. Lett. Ed.* **1973**, *111*, 503.
- (13) Delgado, J.; El-Aasser, M. S.; Vanderhoff, J. W. *J. Polym. Sci., Polym. Sci. Ed.* **1986**, *24*, 861–874.
- (14) Mouran, D.; Reimers, J.; Schorks, J. F. *J. Polym. Sci., Polym. Sci. Ed.* **1996**, *34*, 1073.
- (15) Blythe, P. J.; Morrison, B. R.; Mathauer, K. A.; Sudol, E. D.; El-Aasser, M. S. *Langmuir* **2000**, *16*, 898–904.
- (16) Ugelstad, J.; Mørk, P. C. *Adv. Colloid Interface Sci.* **1980**, *13*, 101–140.
- (17) Gooch, J. W.; Dong, H.; Schork, F.-J. *J. Appl. Polym. Sci.* **2000**, *76*, 105–114.
- (18) Van Hamersveld, E. M. S.; Van Es, J. J. G. S.; Cuperus, F. P. *Colloids Surf., A: Physicochem. Eng. Asp.* **1999**, *153*, 285–296.
- (19) El Aasser, M. S.; Lack, C. D.; Vanderhoff, J. W.; Fowkes, F. M. *Colloids Surf.* **1988**, *29*, 103–118.
- (20) Landfester, K. *Macromol. Symp.* **2000**, *150*, 171–178.
- (21) Delgado, J.; El-Aasser, M. S. *Makromol. Chem., Macromol. Symp.* **1990**, *31*, 63–87.
- (22) Chou, Y. J.; El-Aasser, M. S. *J. Dispersion Sci. Technol.* **1980**, *1* (2), 129–150.
- (23) Landfester, K. *Adv. Mater.* **2001**, *13*, 765–768.
- (24) Davis, S. S.; Round, H. P.; Purewal, T. S. *J. Colloid Interface Sci.* **1981**, *80* (2), 508–511.
- (25) Webster, A. J.; Cates, M. E. *Langmuir* **1998**, *14*, 2068–2079.
- (26) Kabalnov, A. S.; Pertsov, A. V.; Shchukin, E. D. *Colloids Surf.* **1987**, *24*, 19–32.
- (27) Kabalnov, A. S.; Makarov, K. N.; Pertsov, A. V.; Shchukin, E. D. *J. Colloid Interface Sci.* **1990**, *138*, 98–104.
- (28) Welin-Berger, K.; Bergenstahl, B. *Int. J. Pharm.* **2000**, *200*, 249–260.
- (29) Fontenot, K.; Schork, F. J. *J. Appl. Polym. Sci.* **1993**, *49*, 633–655.
- (30) Jabbari, E.; Khakpour, M. *Biomaterials* **2000**, *21*, 2073–2079.
- (31) Hong, K.; Park, S. *React. Funct. Polym.* **1999**, *42*, 193–200.
- (32) Landfester, K.; Willert, M.; Antonietti, M. *Macromolecules* **2000**, *33*, 2370–2376.
- (33) Soto-Portas, M. L. PhD Thesis, Lyon, France, 2003.
- (34) Shanta, K. L.; Panduranga Rao, K. *J. Appl. Polym. Sci.* **1993**, *50*, 1863–1870.
- (35) Hong, K.; Park, S. *Mater. Sci. Eng. A* **1999**, *A272*, 418–421.
- (36) Kojio, K.; Fukumaru, T.; Furukawa, M. *Macromolecules* **2004**, *37*, 3287–3291.
- (37) Lan, P. N.; Corneillie, S.; Schacht, E.; Davies, M.; Shard, A. *Biomaterials* **1996**, *17*, 2273–2280.
- (38) Schriener, D. C.; Wittal, R. M.; Li, L. *Macromolecules* **1997**, *30*, 1955–1963.
- (39) Beyou, E.; Chaumont, P.; Chauvin, F.; Devaux, C.; Zydowicz, N. *Macromolecules* **1998**, *31*, 6828–6835.

MA047808E